EIF3D silencing suppresses renal cell carcinoma tumorigenesis via inducing G2/M arrest through downregulation of Cyclin B1/CDK1 signaling

XIU-WU PAN[1,2*], LU CHEN[1*], YI HONG[3], DAN-FENG XU[4], XI LIU[1], LIN LI[1,2], YI HUANG[1], LI-MING CUI[4], SI-SHUN GAN[2], QI-WEI YANG[1,2], HAI HUANG[1], FA-JUN QU[2], JIAN-QING YE[2], LIN-HUI WANG[1] and XIN-GANG CUI[2]

[1]Department of Urinary Surgery of Changzheng Hospital, Second Military Medical University, Shanghai 200003; [2]Department of Urinary Surgery of Third Affiliated Hospital, Second Military Medical University, Shanghai 201805; [3]Duruo Biotechnologies Inc., Shanghai 200233; [4]Department of Urinary Surgery of Ruijin Hospital, Shanghai Jiaotong University, Shanghai 200025, P.R. China

Received February 2, 2016; Accepted March 10, 2016

DOI: 10.3892/ijo.2016.3459

Abstract. There are no effective therapies for advanced renal cell carcinoma (RCC), except for VEGFR inhibitors with only ~50% response rate. To identify novel targets and biomarkers for RCC is of great importance in treating RCC. In this study, we observed that eukaryotic initiation factor 3d (EIF3D) expression was significantly increased in RCC compared with paracarcinoma tissue using immunohistochemistry staining and western blot analysis. Furthermore, bioinformatics meta-analysis using ONCOMINE microarray datasets showed that EIF3D mRNA expressions in CCRCC tissue specimens were significantly higher than that in normal tissue specimens. In addition, RCC tissue microarray demonstrated that elevated EIF3D expression was positively correlated with TNM stage and tumor size. EIF3D silencing in human 786-O and ACHN CCRCC cell lines by RNA interference demonstrated that EIF3D knockdown obviously inhibited cell proliferation and colony formation, caused G2/M arrest through down-regulation of Cyclin B1 and Cdk1 and upregulation of p21, and induced apoptosis shown by sub-G1 accumulation and RARP cleavage. Moreover, correlation analysis using ONCOMINE microarray datasets indicated that increased EIF3D mRNA expression was positively correlated to PCNA, Cyclin B1 and CDK1 mRNA expression in RCC. Collectively, these results provide reasonable evidences that EIF3D may function as a potential proto-oncogene that participates in the occurrence and progression of RCC.

Correspondence to: Dr Xin-Gang Cui, Department of Urinary Surgery of Third Affiliated Hospital, Second Military Medical University, Shanghai 201805, P.R. China
E-mail: xingangcui@126.com

Dr Lin-Hui Wang, Department of Urinary Surgery of Changzheng Hospital, Second Military Medical University, Shanghai 200003, P.R. China
E-mail: wlhui@medmail.com.cn

*Contributed equally

Key words: renal cell carcinoma, eukaryotic initiation factor 3d, tumor growth, Cyclin B1, CDK1

Introduction

Renal cell carcinoma (RCC) has been identified as the most commonly diagnosed subtype of kidney cancer, accounting for 2-3% of all malignancies (1). According to specific histopathological and genetic characteristics, three common pathologic types of RCC, including clear cell RCC (CCRCC; 80-90%), papillary RCC (PRCC; 10-15%) and chromophobe RCC (CRCC; 4-5%) account for 90% of all RCCs (2). At present, radical nephrectomy is an effective treatment for early-stage and localized RCC (3). However, there are still a certain part of patients diagnosed with advanced or metastatic RCC (mRCC) at the first visit (4). Some patients, although they have a small and localized RCC at the beginning, may still develop metastatic RCC after radical nephrectomy, where the underlying mechanisms are poorly understood. Therefore, it is urgent to develop novel biomarkers for early diagnosis and prognostic assessment. Although with the progress of molecular biology, neoadjuvant therapy targeting VEGFR (5) has brought a new hope for advanced mRCC, original drug resistance was seen in ≥50% of the patients, and acquired drug resistances were developed monthly. Therefore, an increasing understanding of the complex molecular basis of RCC is needed for the clinical treatment of this aggressive malignancy.

Translation of mRNA is a key process for protein synthesis in eukaryotes, including initiation, elongation and termination. Regulation of protein synthesis at translation initiation level is essential for the control of cell proliferation under normal physiological conditions. Eukaryotic translation initiation factor 3 (eIF3) is the largest known multi-protein complex containing 13 subunits (EIF3A-EIF3M), and is required for

eukaryotic protein synthesis by binding mRNA to 40S small ribosomal subunits and preventing premature binding of large ribosomal subunits (6). Interestingly, misregulation of EIF3 expression is closely related to cancer development and progression (6). It was recently reported (7) that over-expression of eIF3a could promote the growth of ovarian cancer cells and decrease the sensitivity of ovarian cancer cells to cisplatin. In addition, increased eIF3e expression was reported to be associated with colon tumor development and poor prognosis, whereas knockdown of eIF3e inhibited the proliferation of colon cancer cells (8). EIF3D, one of the core subunits of eIF3, was reported to play an oncogenic role in prostate cancer, glioma, melanoma, colon cancer and non-small cell lung cancer (NSCLC) (9-13). However, the clinical significance and biological function of eIF3 in human RCC remains unclear.

Therefore, the objective of this study was to explore the role of EIF3D in the pathogenesis of RCC, through IHC staining of RCC specimens, oncomine dataset analysis, and shRNA-mediated gene knockdown. The possible molecular mechanism involved in EIF3D-mediated function was also investigated.

Materials and methods

Cancer specimens and tissue microarray. In total 20 CCRCC tissue specimens and corresponding paired paracarcinoma tissue specimens were provided by the Department of Urinary Surgery of Shanghai Changzheng Hospital from January 2015 to June 2015. All specimens were fixed in formalin and embedded with paraffin. RCC tissue specimens and corresponding paired paracarcinoma tissue specimens were snap frozen in liquid nitrogen and stored at -80˚C before use. None of the patients had other renal diseases, other tumors or systemic diseases, and did not undergo any surgery before the radical nephrectomy. RCC tissue microarray containing 102 RCC specimens were obtained from the Department of Urinary Surgery of Shanghai Changhai Hospital. Of the 102 RCC specimens, 92 were CCRCC, 6 were PRCC and the remaining 4 specimens were CRCC. This study was approved by the institutional review board of the Second Military Medical University (Shanghai, China). All the patients were required to provide written informed consent before enrollment.

Cell lines. Human CCRCC cell lines 786-O, ACHN, A498, 769-P, Caki-1 and Caki-2 were obtained from the cell bank of the Chinese Academy of Sciences (Shanghai, China). 786-O and 769-P cell lines were maintained in RPMI-1640 (Hyclone) with 10% fetal bovine serum (FBS, Gibco). ACHN cell line was maintained in DMEM (Hyclone) with 10% FBS (Gibco). Caki-1, A498 and Caki-2 cell lines were maintained in MEM (Hyclone) with 10% FBS (Gibco). All of these cells were cultured in a humidified incubator containing 5% CO_2 at 37˚C.

Immunohistochemistry. Paraffin blocks were sliced into 5-μm sections, and sequentially dewaxed in xylene, 100, 90, 80 and 70% ethanol and ddH_2O. The slides were first incubated with rabbit anti-EIF3D antibody (1:200, ab155419, Abcam) at 4˚C overnight, labeled with biotinylated goat anti-rabbit serum and streptavidin-peroxidase conjugate for 15 min, and developed with diaminobenzidine (DAB). The positivity and intensity were assessed under a light microscope by two independent pathologists in a blinded manner. The distribution area (0, 0-20, 20-60 and 60-100%) of EIF3D-positive staining cells was given 0, 1, 2 and 3 scores, respectively. The specimen staining intensities, which were light yellow, yellow, brown yellow and reddish brown, were given 0, 1, 2 and 3 scores, respectively. The final score was a combination of the two scores, classified into four grades: negative (0), weak (1), medium (2-4), and strong (5-6), respectively.

Lentivirus construction and transfection. ShRNA sequence targeting human EIF3D (NM_003753.3) (5'-GCGTCATTGA CATCTGCATGACTCGAGTCATGCAGATGTCAATGACG CTTTTTT-3') and the control shRNA sequence (5'-CTAGCC CGGTTCTCCGAACGTGTCACGTATCTCGAGATACGTG ACACGTTCGGAGAATTTTTTTAAT-3') were designed and inserted into the plasmid pFH vector (Hollybio, Shanghai, China) containing green fluorescent protein (GFP) as a reporter gene. To generate recombinant lentivirus, the reconstructed EIF3D silencing plasmid and two packaging plasmids were cotransfected into HEK293T cells using calcium phosphate precipitation method. Approximately 72 h after transfection, recombinant lentivirus was harvested and purified by ultracentrifugation. For lentiviral transduction, 786-O cells ($3x10^4$ cell/well) and ACHN cells ($6x10^4$ cell/well) were seeded in 6-well plates overnight, and transduced with lentivirus containing shEIF3D or shCon at MOIs of 25 and 20, respectively. Transduction efficiency was monitored by relative GFP expression under fluorescent microscopy at 72 h post-transduction. At 120 h after transduction, cells were harvested to verify EIF3D silencing efficiency using RT-PCR and western blotting.

Quantitative real-time PCR. Total RNA was isolated from cells and samples using TRIzol reagent (Gibco) according to the manufacturer's instructions. Total RNA (2 μg) was reverse transcribed into cDNA using oligo(dT) primer and the M-MLV reverse transcriptase (Promega). Total 10 μl 2X SYBR premix ex-taq, 0.5 μl primer, 5 μl cDNA and 4.5 μl ddH_2O were mixed for quantitative real-time PCR (qRT-PCR) using CFX Connect™ Real-Time PCR Detection System (Takara). The primer sequences used were: 5'-CTGGAGGAGGGCAAA TACCT-3' (forward) and 5'-CTCGGTGGAAGGACAAA CTC-3' (reverse) for EIF3D; 5'-GTGGACATCCGCAAA GAC-3' (forward) and 5'-AAAGGGTGTAACGCAACTA-3' (reverse) for β-actin. The $2^{-\Delta\Delta Ct}$ method was used to calculate relative expression level of EIF3D, being normalized to β-actin. The experiment was performed in triplicate and repeated three times.

Western blotting. Cell samples and fresh RCC tissues were lysed in 2X SDS lysis buffer at 4˚C and boiled for 5 min. Then, the supernatant was separated by centrifugation at 12,000 x g for 10 min at 4˚C. Protein quantification was carried out using BCA protein assay kit. Proteins after quantification were separated in 10% SDS-PAGE gel electrophoresis and transferred onto PVDF membranes. Next, the transferred PVDF membranes were blocked in 5% non-fat milk dissolved

in TBST solution for 1 h at room temperature. Then, the membrane was probed with the following primary antibodies: EIF3D (ab155419, Abcam), RARP (#9542, Cell Signaling), Cyclin B1 (#21540, SAB), CDC2 (#19532-1-AP, Proteintech), P21 (#2947, Cell Signaling) and GAPDH (#10494-1-AP, Proteintech) at 4˚C overnight, and then incubated with horseradish peroxidase-conjugated goat anti-rabbit IgG antibody (#Sc-2054, Santa Cruz) for 1 h at room temperature. The signals of proteins were detected with enhanced chemiluminescence. GAPDH protein was used as an internal control.

MTT assay. Cell viability after EIF3D knockdown was measured using 3-(4, 5-dimethylthiazol-2-yl)-2,5-diphenyltetrazolium bromide (MMT) assay. After 72-h infection, 786-O and ACHN cells from different groups (Con, Lv-shCon, Lv-shEIF3D) were trypsinized, suspended, counted and plated in a 96-well plate at a density of $3x10^3$ cells/well for five points in time (days 1, 2, 3, 4 and 5). At each time-point, cells were incubated with MTT solution for 4 h and then incubated with acidified isopropanol overnight. The absorbance at 595 nm was measured using microplate reader. The experiment was performed three times and each group sample had five repetitions.

Plate colony formation assay. After 72-h infection, 786-O and ACHN cells from different groups (Con, Lv-shCon, Lv-shEIF3D) were trypsinized, suspended, counted and plated in a 6-well plate at a density of 400 cells/well. Subsequently, culture medium was replaced every 3 days. After incubation for 2 weeks, cells were fixed in 4% paraformaldehyde for 30 min, and stained with Giemsa solution for 20 min. The number of colonies (>50 cells per colony) in each well was counted under a light microscope and photographed using a digital camera. The experiment was performed three times and each group had three repetitions.

Cell cycle analysis. After 120-h infection, 786-O and ACHN cells from different groups (Con, Lv-shCon, Lv-shEIF3D) were trypsinized, centrifuged, washed with ice-cold PBS, fixed in 75% ethanol overnight, washed again with PBS, centrifuged, and incubated in 500 μl PI staining solution (PI and RNase A) at 37˚C for 1 h. Cell cycle distribution was analyzed by flow cytometer (BD Biosciences, USA). The experiment was performed three times in triplicate.

Bioinformatics meta-analysis using ONCOMINE microarray datasets. To investigate the expression of EIF3D in RCC tissue vs. normal kidney tissue, we conducted a meta-analysis on online microarray data in the Oncomine database (www.onocomine.org) including previously published and publicly available 715 datasets and 86,733 samples. The following search terms were used: 'EIF3D', 'Cancer vs. Normal Analysis', 'Kidney Cancer' and 'mRNA'. Then, six datasets were identified. One dataset (Cutcliffe Renal, Clin Cancer Res, 2005) that did not include a differential analysis of RCC vs. normal kidney was excluded from our meta-analysis. All data are reported Log2 Median-Centered intensity in the Oncomine database. Correlation analysis of two gene expressions was performed on the same dataset (Jones Renal, Clin Cancer Res, 2005).

Table I. IHC staining of EIF3D expression in prostate cancer and paired paracarcinoma tissues.

	No. of specimen	Positive level			P-value[a]
		+/-	+	++	
Cancer	20	0	5	15	<0.001
Paracancerous	20	8	10	2	

[a]Wilcoxon signed rank text.

Statistical analysis. All results were drafted in diagrams by GraphPad Prism 5 software. Wilcoxon signed rank test was carried out to evaluate differences in EIF3D expression between RCC tissue and paired paracarcinoma tissue. Chi-square test was used to analyze EIF3D expression and patient characteristics of RCC tissue microarray. Statistical comparisons on the continuous variables of two groups (Lv-shCon vs. Lv-shEIF3D) were performed by the Student's t-test. All statistical calculations were carried out using SPSS version 19 (IBM Corp., USA), and P-value <0.05 was considered statistically significant.

Results

EIF3D mRNA and protein are upregulated in RCC tissue. To compare the expression levels of EIF3D in clinical RCC tissue and paired paracarcinoma tissue, three pairs of fresh RCC tissues and paired paracarcinoma tissues were analyzed by western blotting. It was found that the EIF3D expression level in RCC tissue was significantly higher than that in the paracarcinoma tissues (P=0.005) (Fig. 1A and B). Representative images of EIF3D staining are shown in Fig. 1C. Moreover, EIF3D expressions in RCC tissues was also significantly higher than that in the paracarcinoma normal kidney tissues (Fig. 1D), and the difference was considered to be statistically significant (Table I, P<0.001).

Correlations between EIF3D expression and clinicopathologic features in RCC patients. To further confirm the clinical significance of EIF3D in RCC, an RCC tissue microarray containing 102 cases of RCC sections were used to assess the relationships between EIF3D proteins and corresponding patient clinicopathological features by Chi-square test. As shown in Table II, EIF3D expression in RCC tissues was significantly correlated with tumor size (P=0.004) and TNM stage (P=0.03), while no significant associations were observed between EIF3D expression and sex, age, Fuhrman grade, histologic type or metastasis. Notably, the percentage of EIF3D staining intensity was positively correlated with the TNM stage (Fig. 1E and F).

Knockdown of EIF3D in RCC cells through lentivirus-mediated expression of shRNA. Considering that EIF3D was upregulated in RCC and correlated to tumor stage, we further explored the cellular functions of this protein in

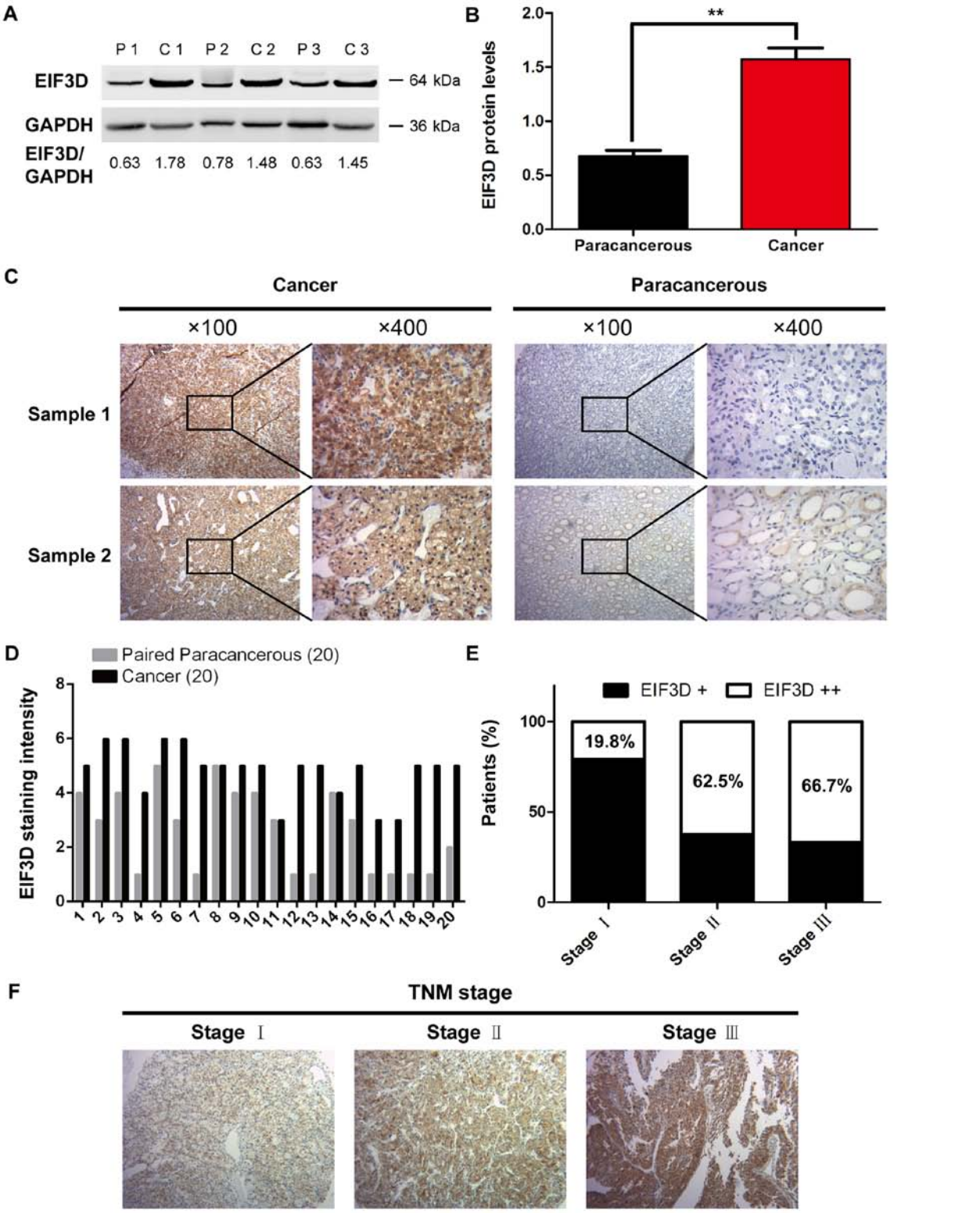

Figure 1. EIF3D expression is upregulated in RCC tissues. (A and B) Western blot analysis was performed in three cases of fresh CCRCC tissues and paired paracarcinoma tissues. (C) Representative immunohistochemical images are presented of EIF3D expression in CCRCC and paired paracarcinoma tissues. (D) EIF3D expression is significantly higher in the CCRCC tissue than that in the paired paracarcinoma tissue (***P<0.001). (E) Statistical analysis of EIF3D staining intensity among different TNM stages. (F) Representative images of EIF3D-positive staining of different TNM stages.

RCC cell lines. Consistent with the findings in RCC tissues, the expression of EIF3D protein was overexpressed in RCC cell lines, including A498, 769-P, 786-O, ACHN, Caki-1 and Caki-2 (Fig. 2A). Two RCC cell lines, 786-O and ACHN cell lines, with relatively higher EIF3D expression were selected for loss-of-function study. Lentivirus-introduced shRNA was used to silence EIF3D expression in 786-O and ACHN cells. As shown in Fig. 2B, most of the cells presented GFP-positive signals of >90% under fluorescence microscopy, indicating successful infection efficiency. To further determine EIF3D

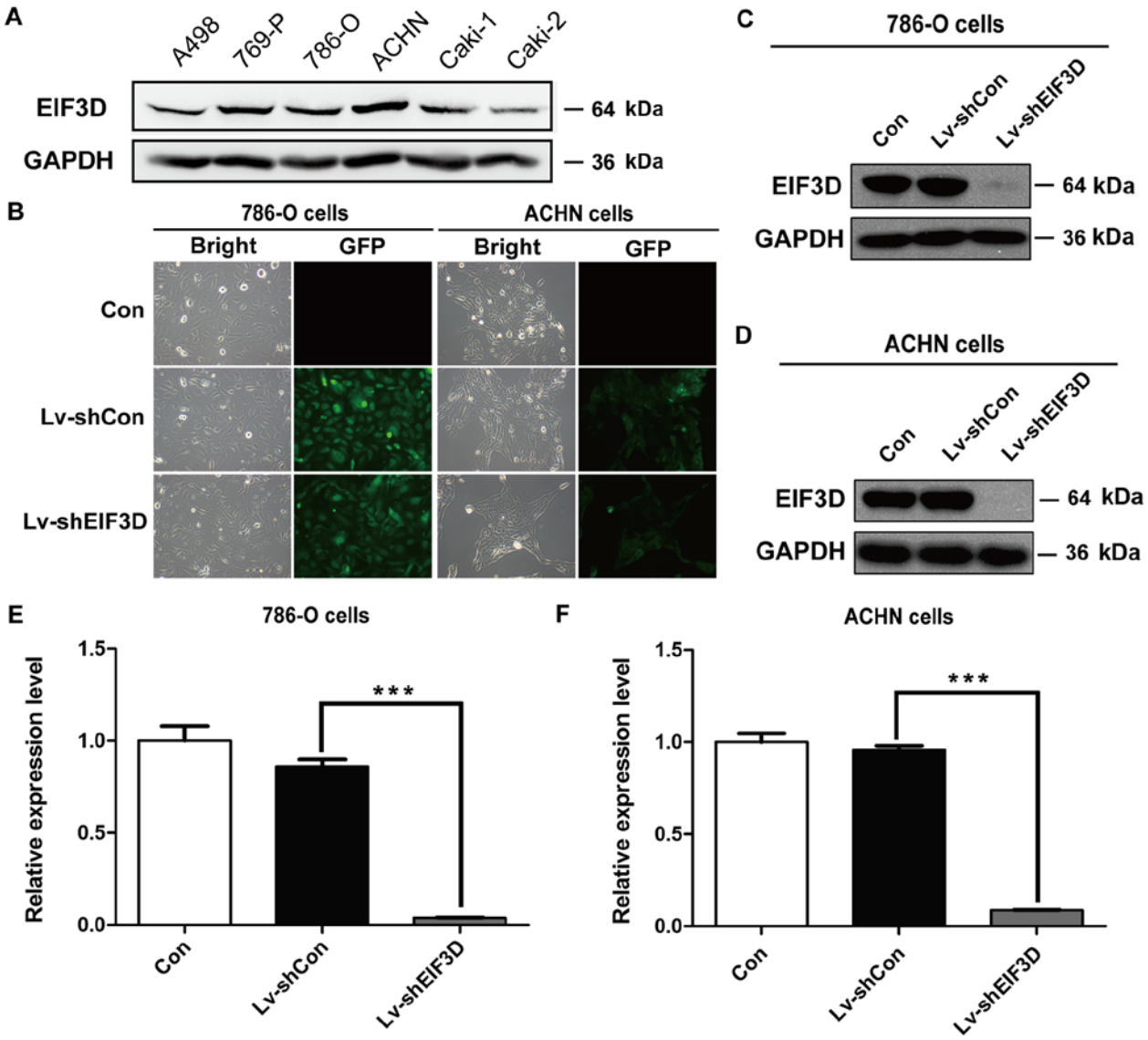

Figure 2. Determination of the transduction and silencing efficiency of lentivirus mediated RNA interference against EIF3D in 786-O and ACHN cells. (A) A498, 769-P, 786-O, ACHN, Caki-1 and Caki-2 cell lines were used to analyze EIF3D expression by western blot analysis. (B) The infection efficiency was determined by light and fluorescence microscopy 72 h after infection in Con, Lv-shCon and Lv-shEIF3D. (C and D) Western blot analysis in 786-O and ACHN cells showed that EIF3D protein expression in Lv-shEIF3D group was significantly higher than that in con and Lv-shCon group. (E and F) RT-PCR showed that EIF3D mRNA expression in Lv-shEIF3D group was significantly inhibited as compared with that in con and Lv-shCon group (***P<0.001).

silencing efficiency, the level of EIF3D protein and mRNA was analyzed through RT-PCR and western blotting in the 786-O and ACHN cells after EIF3D knockdown. As shown in Fig. 2C and D, EIF3D protein expression in Lv-shEIF3D group of the two cell lines was significantly suppressed as compared with those in Lv-shCon group. In addition, the mRNA levels of EIF3D were significantly reduced by 95.5% in 786-O cells and 91.1% in ACHN cells after EIF3D knockdown (Fig. 2E and F, P<0.001), suggesting that shRNA targeting EIF3D successfully inhibited gene expression.

Knockdown of EIF3D impaired RCC cell proliferation and colony formation ability. To investigate the function of EIF3D in RCC cells, we examined whether reduction of EIF3D expression has an effect on cell proliferation and colony formation ability. MTT assay was used to measure cell viability in 786-O and ACHN cells after knockdown of EIF3D. As shown in Fig. 3A and B, the growth curves of 786-O and ACHN cells remarkably declined upon EIF3D knockdown. The number of viable cells was greatly reduced in Lv-shEIF3D groups than that in Lv-shCon groups in 786-O and ACHN cells (P<0.001). Moreover, cell colony formation assay was performed to gain additional insight into the effect of EIF3D on malignant proliferation of RCC cells. There was a significant difference in the colony sizes between Lv-shEIF3D group and Lv-shCon group (Fig. 3C), especially in 786-O cell line. The number of colonies of the two RCC cell lines was decreased significantly in Lv-shEIF3D group as compared with that in Lv-shCon group (786-O cells: 0.0±0.0 vs. 83.0±2.0, P=0.001; ACHN cells: 19.0±2.0 vs. 85.0±2.6, P<0.001) (Fig. 3C and D). These results indicated that EIF3D plays a vital role in the malignant growth of RCC cells.

Table II. Correlations between EIF3D expression and clinicopathologic parameters in patients with RCC using tissue microarray analysis.

Parameters	Total (n=102)	Expression of EIF3D + (n=77, %)	Expression of EIF3D ++ (n=25, %)	P-value (Chi-square test)
Gender				
Male	71 (69.6)	56 (72.7)	15 (60.0)	0.229
Female	31 (30.4)	21 (27.3)	10 (40.0)	
Tumor size (cm)				0.004[a]
≤4	58 (56.9)	50 (64.9)	8 (32.0)	
>4	44 (43.1)	27 (35.1)	17 (68.0)	
TNM stage				0.03[a]
I	91 (89.2)	73 (94.8)	18 (72.0)	
II	8 (7.8)	3 (3.9)	5 (20.0)	
III	3 (2.9)	1 (1.3)	2 (8.0)	
Fuhrman grade				0.269
1	35 (34.3)	28 (36.4)	7 (28.0)	
2	55 (53.9)	40 (51.9)	15 (60.0)	
3	11 (10.9)	9 (11.7)	2 (8.0)	
4	1 (1.0)	0	1 (4.0)	
Histology				0.355
CCRCC	92 (90.2)	68 (88.3)	24 (96.0)	
PRCC	6 (5.9)	6 (7.8)	0	
CRCC	4 (3.9)	3 (3.9)	1 (4.0)	
Metastases				0.314
Yes	6 (5.9)	3 (3.9)	3 (12.0)	
No	96 (94.1)	74 (96.1)	22 (88.0)	

CCRCC, clear cell renal cell carcinoma; PRCC, papillary renal cell carcinoma; CRCC, chromophobe renal cell carcinoma.

Silencing of EIF3D induces G2/M phase arrest in RCC cells. To explore the potential mechanism underlying the suppressive effect of EIF3D silencing on tumor cell proliferation, cell cycle distribution was evaluated using flow cytometry. As shown in Fig. 4A and C and E, knockdown of EIF3D in 786-O and ACHN cells significantly increased the percentage of cells in G2/M phase (786-O cells: 39.33±1.27 vs. 15.74±1.28%, P<0.001; ACHN cells: 56.04±0.92 vs. 19.70%±0.43%, P<0.001) and decreased the percentage of cells in G0/G1 phase (786-O cells: 32.85±0.34 vs. 54.00±0.61%, P<0.001; ACHN cells: 31.27±0.48 vs. 49.31±0.64%, P<0.001). Moreover, the number of S-phase ACHN cells treated with Lv-shEIF3D was also markedly decreased (12.69±0.48 vs. 30.99±0.35%, P<0.001). Besides, more cells were accumulated in sub-G1 phase in 786-O and ACHN cells after EIF3D knockdown as compared with the control (786-O cells: 6.09±0.36 vs. 1.67±0.48%, P=0.001; ACHN cells: 1.76±0.25 vs. 0.46±0.30%, P=0.01) (Fig. 4D and F), suggesting that knockdown of EIF3D might induce cell apoptosis.

To further understand the mechanism underlying G2/M phase arrest, the expression alterations of cell cycle regulators were detected in 786-O and ACHN cells after EIF3D knockdown using western blot analysis. As shown in Fig. 4B, the expression levels of CDK1 and Cyclin B1, associated with G2-M transition, were decreased in Lv-shEIF3D groups, whereas the expression levels of p21 and RARP cleavage were increased in 786-O and ACHN cells following Lv-shEIF3D transduction.

Meta-analysis of EIF3D expression in RCC vs. normal kidney tissues using ONCOMINE microarray database. To further confirm our findings that EIF3D is overexpressed in RCC, public microarray datasets from ONCOMINE database were used to carry out meta-analysis of EIF3D gene expression. A total of five online microarray datasets containing mRNA level test of cancer vs. normal tissue were included in our study, which contains 136 CCRCC and 58 normal kidney tissues. As shown in Table III, EIF3D was significantly overexpressed in the CCRCC samples in Jones, Beroukhim,

Table III. EIF3D expressions in ONCOMINE microarray datasets.

Dataset	Subtype	N (cancer/ normal)	P-value[a] (cancer/ normal)	Fold change (cancer/ normal)	% Gene ranking	Database references
Jones	CCRCC	32/23	5.14E-12	1.824	572	Clin Cancer Res 2005/08/15
	PRCC	11/23	7.32E-06	1.637	1,552	
	CRCC	6/23	0.326	1.076	7,495	
Beroukhim	Hereditary CCRCC	32/11	3.08E-07	1.393	1,059	Cancer Res 2009/06/01
	Non-hereditary CCRCC	27/11	1.32E-04	1.286	1,731	
Lenburg	CCRCC	9/9	0.007	1.323	2,052	BMC Cancer 2003/11/27
Cumz	CCRCC	10/10	0.004	1.321	2,139	Clin Cancer Res 2007/08/15
Yusenko	CCRCC	26/5	0.105	1.339	7,645	BMC Cancer 2009/05/18
	PRCC	19/5	0.127	1.236	8,673	
	CRCC	4/5	0.127	1.542	8,039	

RCC, clear cell renal cell carcinoma; PRCC, papillary renal cell carcinoma; CRCC, chromophobe renal cell carcinoma. [a]Student's t-test.

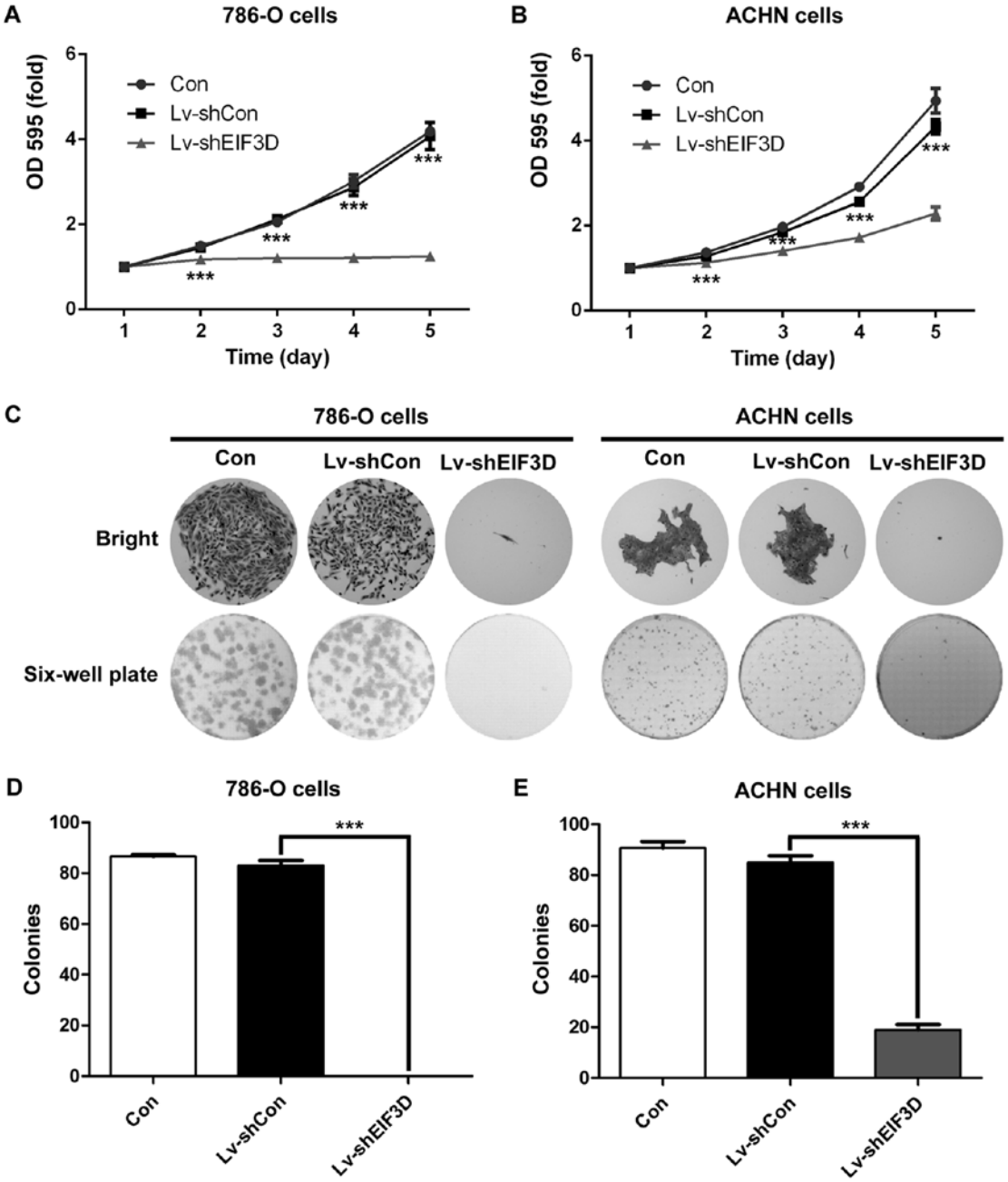

Figure 3. Silencing of EIF3D downregulates the proliferation and colony formation ability of 786-O and ACHN cells. (A and B) MTT assay showed significant differences in the proliferation of 786-O and ACHN cells between Lv-shEIF3D and con and Lv-shCon groups. (C) Representative light microscopic images regarding the size and number of colonies. (D and E) The number of colonies in Lv-shEIF3D group was significantly lower than the con and Lv-shCon group (***P<0.001).

Lenburg and Cumz datasets, and slightly upregulated CCRCC samples in Yusenko datasets. Meta-analysis of the five datasets collectively revealed that increased EIF3D mRNA expression was associated with CCRCC as compared with the normal kidney tissue (gene median rank: 1891.5, P=0.004) (Fig. 5A). In the Beroukhim renal microarray dataset, EIF3D mRNA expression in CCRCC containing hereditary CCRCC and non-hereditary CCRCC exhibited a significant difference as compared with the normal tissue (P<0.001) (Fig. 5B). To study whether EIF3D is differentially expressed in distinct RCC subtypes, Jones renal dataset (Fig. 5C) was further analyzed. It was found that RCC tended to have higher EIF3D expression than renal oncocytoma, a benign renal tumor (P=0.187) (Fig. 5D). Among RCCs, CCRCC had significantly higher EIF3D expression than CRCC and PRCC (Fig. 5E, CCRCC vs. PRCC: P=0.01; CRCC vs. PRCC: P=0.05; CCRC vs. CRCC: P=0.157).

EIF3D is positively correlated with PCNA, Cyclin B1 and CDK1. We also investigated the correlation of EIF3D and potential downstream signaling molecules using ONCOMINE datasets. As depicted in Fig. 6, EIF3D was positively correlated with PCNA, a proliferative biomarker (r^2=0.1687, P<0.0001), suggesting a correlation of EIF3D with the malignant growth of RCC. In addition,

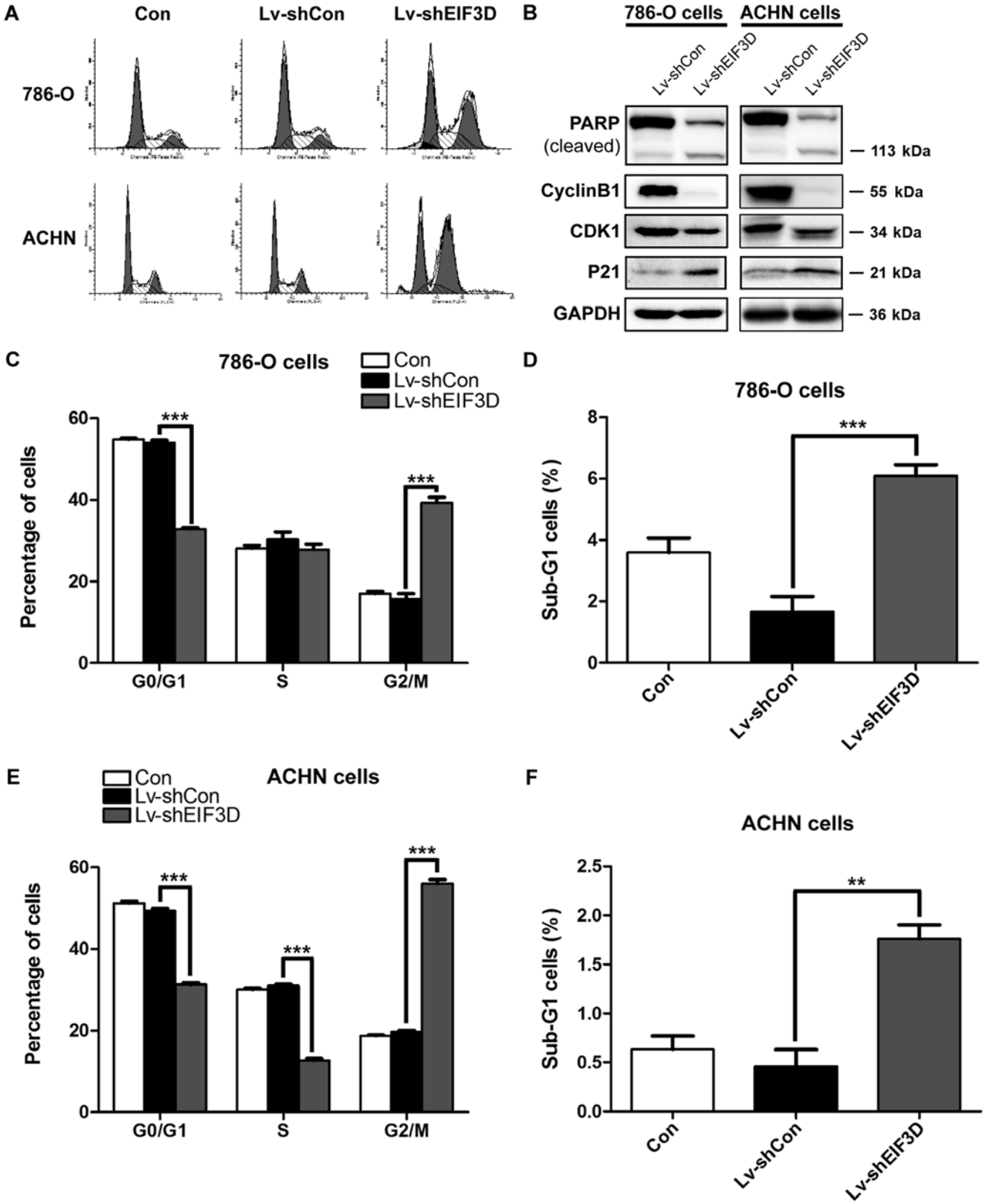

Figure 4. EIF3D knockdown induces G2/M phase arrest and apoptosis of 786-O and ACHN cells. (A) The percentage of cell cycle distribution was analyzed using flow cytometry. (C and E) Statistical analysis showed that more cells were arrested at G2/M phase in Lv-shEIF3D group as compared with the control group (***P<0.001). (D and F) Statistical analysis showed that the rate of apoptotic cell accumulation in Lv-shEIF3D group was significantly higher than that in the control group (**P<0.01; ***P<0.001). (B) Differences in protein expression level of Cyclin B1, CDK1, P21 and RARP (cleaved) between Lv-shEIF3D and Lv-shCon groups were determined by western blotting.

EIF3D expression was also positively correlated with Cyclin B1 (r^2=0.2354, P<0.0001) and CDK1 (r^2=0.1332, P=0.0003) expressions in RCC, providing evidence at the *in vivo* level that EIF3D may regulate cell cycle progression in RCC.

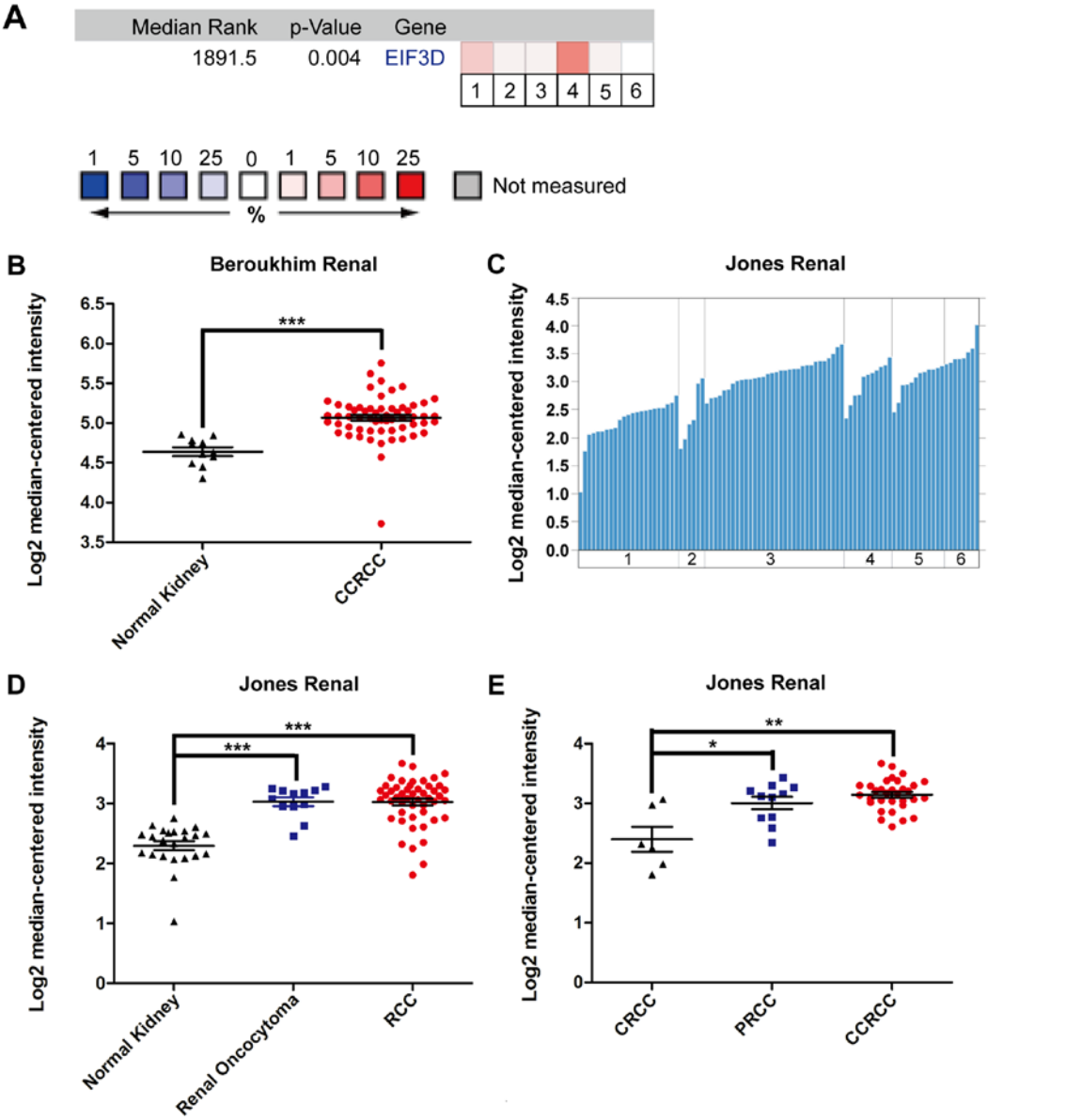

Figure 5. EIF3D mRNA expression in CCRCC vs. normal kidney tissues was analyzed by using ONCOMINE microarray database. (A) Five microarray datasets regarding EIF3D mRNA expression in CCRCC vs. normal tissues were included in our meta-analysis: 1-2, Beroukhim Renal (hereditary CCRCC and non-hereditary); 3, Gumz Renal; 4, Jones Renal; 5, Lenburg Renal; 6, Yusenko Renal. Data are shown as the median rank of IF3d through each dataset analysis. P-value for EIF3D is presented using the median ranked analysis on CCRCC vs. normal tissues. (B) Beroukhim renal microarray dataset showed that EIF3D mRNA expression in CCRCC was significantly upregulated compared with the normal tissue (***P<0.001). Data are presented as log2 median-centered intensity. (C-E) Differential expression of EIF3D mRNA expression in several common tissue subtypes was analyzed in Jones independent renal microarray dataset (*P<0.05, **P<0.01; ***P<0.001).

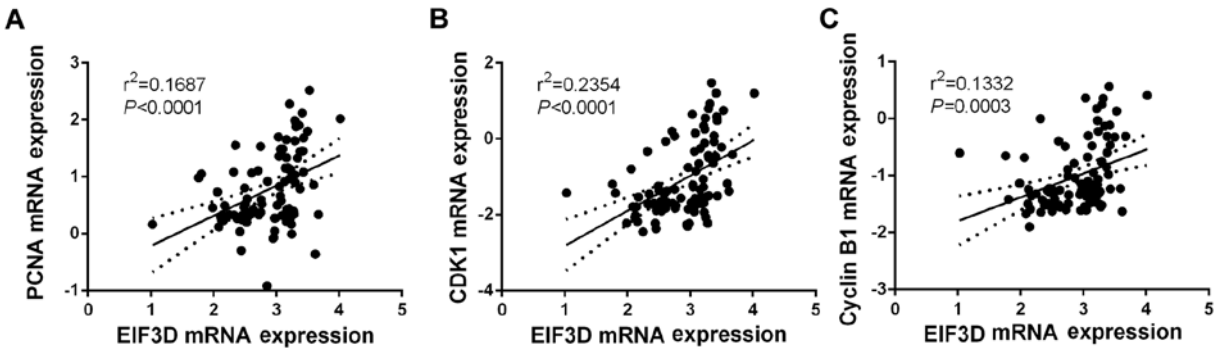

Figure 6. Correlation analysis of EIF3D expression and relevant gene expression using Jones independent renal microarray dataset. (A-C) Increased EIF3D mRNA expression was positively correlated with PCNA, Cyclin B1 and CDK1 mRNA expression. Correlation coefficient of r^2 and P-value are shown in images. Data are presented as log2 median-centered intensity.

Discussion

Gene transcription and mRNA translation are two indispensable processes of eukaryotic gene expression. When eukaryotic mRNA translation is out of control, the process of gene expression will be deregulated, resulting in uncontrolled cell growth or even leading to tumor formation (14). Hence, targeting abnormal translation factors in human cancers may be a potential targeted treatment strategy. EIF3D, as a subunit of EIF3 complex, has been reported to participate in nearly all stages of translation and associated with various cancers. However, its clinical significance and cellular functions in RCC has not been reported yet. Here, we observed that EIF3D was overexpressed in RCC tissues, especially in CCRCC specimens, and that EIF3D expression was positively correlated with malignant features of RCC. Silencing EIF3D by shRNA inhibited malignant growth of 786-O and ACHN RCC cell lines, caused G2/M arrest, and induced apoptosis, through misregulation of cell cycle regulators. These results suggested that increased EIF3D expression was associated with malignant transformation of RCC, and may serve as a biomarker for RCC.

CCRCC is the major histologic subtype of RCC, also called conventional RCC, accounting for >80% RCC (15). There are no effective therapies for advanced mCCRCC, except for VEGFR inhibitors with about only 50% response rate. To identify novel targets and biomarkers for RCC is of great importance in treating RCC. Here, we demonstrated that EIF3D protein expression in RCC tissues was significantly higher than that in the paracarcinoma tissues among 20 clinical specimens. EIF3D mRNA was obviously elevated in 136 CCRCC tissues compared to 58 normal tissues from ONCOMINE database. EIF3D expression in 102 RCC tissue microarray was positively correlated with tumor size (P=0.004) and TNM stage (P=0.03). Moreover, EIF3D expression was significantly increased in CCRCC with a higher malignancy compared with CRCC and PRCC in Jones renal dataset. To further explore the biological function of EIF3D in CCRCC, shRNA was used to knockdown the expression of EIF3D in CCRCC cell lines, 786-O and ACHN cells. Functional analysis indicated that knockdown of EIF3D observably inhibited the capacity of cell proliferation and colony formation, which is in agreement with the effect of EIF3D-silencing observed in prostate cancer, glioma, melanoma, colon cancer and NSCLC cells (9-13). These results implied that EIF3D is a potential proto-oncogene, participating in malignant transformation of RCC.

We found that EIF3D knockdown induced G2/M phase arrest. Consistent with our results, G2/M phase arrest induced by EIF3D knockdown has also been observed in different types of malignant cells (10,11,13,14). However, the potential molecular mechanisms of EIF3D affecting the cell cycle distribution has not yet been reported. G2/M checkpoint in eukaryotic cells is an important cell cycle DNA damage checkpoint, which play an important role in regulating cell cycle progression (16). G2/M arrest is considered to prevent eukaryotic cells from entering the process of mitosis and could be an effective antitumor strategy (17,18). In eukaryotes, cell cycle is regulated by cyclins, cyclin-dependent kinases (CDKs) and cyclin-dependent kinase inhibitors (CDKIs) (19). Cell cycle G2 phase into M phase for mitosis was reported to be regulated by activation of Cyclin B1/Cdk1 complex (19,20). Cyclin-dependent kinase inhibitors (CDKIs) that bind to cyclin/Cdk complexes regulated cell cycle by suppressing the kinase activity of cyclin/Cdk complexes (21). p21, a downstream target of p53 and an important CDKI that induces G2/M phase arrest, was reported to work with proliferating cell nuclear antigen (PCNA)/Cdk complexes to regulate DNA repair (22-24). Our results showed that EIF3D knockdown increased the protein expression of p21 and decreased the protein expression of Cyclin B1 and CDK1, indicating that EIF3D-silencing arrested cell cycle at G2/M phase in CCRCC cells. Furthermore, gene correlation analysis using ONCOMINE microarray database also demonstrated that EIF3D mRNA expression was positively association with the mRNA expression of Cyclin B1, CDK1 and PCNA. These results have been demonstrated by Wu *et al*, who showed that G2/M arrest was attributed to the downregulation of Cyclin B1 and CDK1 and upregulation of p21 (25).

Promoting cell apoptosis is another important mechanism underlying the inhibitory effect of antitumor therapy on the growth of tumor cells (26). Our study demonstrated that silencing of EIF3D markedly induced more cells accumulated in sub-G1 phase in CCRCC cells, suggesting that the percentage of apoptosis cells increased after knockdown of EIF3D. PARP is a vital protein that plays an important role in DNA repair and programmed cell death (27). Once the PARP has been cut by the cleavage of caspases, apoptosis will be induced (28). Western blotting in this study showed that cleaved PARP was upregulated in Lv-shEIF3D group as compared with Lv-shCON group. Recently, it was reported that 5-Nitro-5'-hydroxy-indirubin-3'-oxime (AGM130) induced cell apoptosis through upregulating the level of cleaved PARP to inhibit the growth of A549 NSCLC cells (29). In brief, silencing of EIF3D expression in CCRCC cells increased the production of cleaved PARP to suppress cell growth.

In conclusion, this study provides insights into the clinical significance of EIF3D in RCC, demonstrated that knockdown of EIF3D in RCC cells significantly induced cell growth suppression and cell cycle arrest through down regulation of Cyclin/CDK1 signaling. These results provide reasonable evidence that EIF3D may function as a potential oncogenic molecule that plays a pivotal role in the occurrence and progression of RCC.

Acknowledgements

This study was supported by grants from the National Natural Science Foundation of China for Youths (nos. 81202020 and 81001136); the National Natural Science Foundation of China (no. 81170637); Shanghai Committee of Science and Technology General Program for Medicine (no. 11JC1402302); the Military Fund for Health Care (CWS13BJ09); and the Key Project of Science and Innovation Foundation of Shanghai Ministry of Education (14zz084).

References

1. Siegel R, Naishadham D and Jemal A: Cancer statistics, 2012. CA Cancer J Clin 62: 10-29, 2012.
2. Hes O: International Society of Urological Pathology (ISUP) Vancouver Classification of Renal Neoplasia 2012. Cesk Patol 50: 137-141, 2014 (In Czech).

3. Jiang Z, Chu PG, Woda BA, Liu Q, Balaji KC, Rock KL and Wu CL: Combination of quantitative IMP3 and tumor stage: A new system to predict metastasis for patients with localized renal cell carcinomas. Clin Cancer Res 14: 5579-5584, 2008.
4. Zhao J, Huang X, Sun F, Ma R, Wang H, Shao K, Zhu Y, Zhou W, Xu Z and Shen Z: Prognostic factors for overall survival with targeted therapy in Chinese patients with metastatic renal cell carcinoma. Can Urol Assoc J 8: E821-E827, 2014.
5. Sciarra A, Gentile V, Salciccia S, Alfarone A and Di Silverio F: New anti-angiogenic targeted therapy in advanced renal cell carcinoma (RCC): Current status and future prospects. Rev Recent Clin Trials 3: 97-103, 2008.
6. Spilka R, Ernst C, Mehta AK and Haybaeck J: Eukaryotic translation initiation factors in cancer development and progression. Cancer Lett 340: 9-21, 2013.
7. Zhang Y, Yu JJ, Tian Y, Li ZZ, Zhang CY, Zhang SF, Cao LQ, Zhang Y, Qian CY, Zhang W, *et al*: eIF3a improve cisplatin sensitivity in ovarian cancer by regulating XPC and p27Kip1 translation. Oncotarget 6: 25441-25451, 2015.
8. Li Z, Lin S, Jiang T, Wang J, Lu H, Tang H, Teng M and Fan J: Overexpression of eIF3e is correlated with colon tumor development and poor prognosis. Int J Clin Exp Pathol 7: 6462-6474, 2014.
9. Lin Z, Xiong L and Lin Q: Knockdown of eIF3d inhibits cell proliferation through G2/M phase arrest in non-small cell lung cancer. Med Oncol 32: 183, 2015.
10. Yu X, Zheng B and Chai R: Lentivirus-mediated knockdown of eukaryotic translation initiation factor 3 subunit D inhibits proliferation of HCT116 colon cancer cells. Biosci Rep 34: e00161, 2014.
11. Ren M, Zhou C, Liang H, Wang X and Xu L: RNAi-mediated silencing of EIF3D alleviates proliferation and migration of glioma U251 and U87MG cells. Chem Biol Drug Des 86: 715-722, 2015.
12. Gao Y, Teng J, Hong Y, Qu F, Ren J, Li L, Pan X, Chen L, Yin L, Xu D, *et al*: The oncogenic role of EIF3D is associated with increased cell cycle progression and motility in prostate cancer. Med Oncol 32: 518, 2015.
13. Li H, Zhou F, Wang H, Lin D, Chen G, Zuo X, Sun L, Zhang X and Yang S: Knockdown of EIF3D suppresses proliferation of human melanoma cells through G2/M phase arrest. Biotechnol Appl Biochem 62: 615-620, 2015.
14. Silvera D, Arju R, Darvishian F, Levine PH, Zolfaghari L, Goldberg J, Hochman T, Formenti SC and Schneider RJ: Essential role for eIF4GI overexpression in the pathogenesis of inflammatory breast cancer. Nat Cell Biol 11: 903-908, 2009.
15. Dagher J, Dugay F, Rioux-Leclercq N, Verhoest G, Oger E, Bensalah K, Cabillic F, Jouan F, Kammerer-Jacquet SF, Fergelot P, *et al*: Cytoplasmic PAR-3 protein expression is associated with adverse prognostic factors in clear cell renal cell carcinoma and independently impacts survival. Hum Pathol 45: 1639-1646, 2014.
16. Cuddihy AR and O'Connell MJ: Cell-cycle responses to DNA damage in G2. Int Rev Cytol 222: 99-140, 2003.
17. Hu X, Zhang Z, Liu T, Song L, Zhu J, Guo Z, Cai J and Yu R: Polypeptide fraction from *Arca subcrenata* induces apoptosis and G2/M phase arrest in HeLa cells via ROS-mediated MAPKs pathways. Evid Based Complement Alternat Med 2015: 930249, 2015.
18. Su CC: Tanshinone IIA inhibits gastric carcinoma AGS cells through increasing p-p38, p-JNK and p53 but reducing p-ERK, CDC2 and cyclin B1 expression. Anticancer Res 34: 7097-7110, 2014.
19. Li JP, Yang YX, Liu QL, Pan ST, He ZX, Zhang X, Yang T, Chen XW, Wang D, Qiu JX, *et al*: The investigational Aurora kinase A inhibitor alisertib (MLN8237) induces cell cycle G2/M arrest, apoptosis, and autophagy via p38 MAPK and Akt/mTOR signaling pathways in human breast cancer cells. Drug Des Devel Ther 9: 1627-1652, 2015.
20. Wang J, Wu A, Xu Y, Liu J and Qian X: M(2)-A induces apoptosis and G(2)-M arrest via inhibiting PI3K/Akt pathway in HL60 cells. Cancer Lett 283: 193-202, 2009.
21. King KL and Cidlowski JA: Cell cycle regulation and apoptosis. Annu Rev Physiol 60: 601-617, 1998.
22. Boonstra J and Post JA: Molecular events associated with reactive oxygen species and cell cycle progression in mammalian cells. Gene 337: 1-13, 2004.
23. Michieli P, Chedid M, Lin D, Pierce JH, Mercer WE and Givol D: Induction of WAF1/CIP1 by a p53-independent pathway. Cancer Res 54: 3391-3395, 1994.
24. Abbas T and Dutta A: p21 in cancer: Intricate networks and multiple activities. Nat Rev Cancer 9: 400-414, 2009.
25. Wu CF and Efferth T: Miltirone induces G2/M cell cycle arrest and apoptosis in CCRF-CEM acute lymphoblastic leukemia cells. J Nat Prod 78: 1339-1347, 2015.
26. Abaza MS, Orabi KY, Al-Quattan E and Al-Attiyah RJ: Growth inhibitory and chemo-sensitization effects of naringenin, a natural flavanone purified from *Thymus vulgaris*, on human breast and colorectal cancer. Cancer Cell Int 15: 46, 2015.
27. Piskunova TS, Yurova MN, Ovsyannikov AI, Semenchenko AV, Zabezhinski MA, Popovich IG, Wang ZQ and Anisimov VN: Deficiency in poly(ADP-ribose) polymerase-1 (PARP-1) accelerates aging and spontaneous carcinogenesis in mice. Curr Gerontol Geriatr Res 2008: 754190, 2008.
28. Ghavami S, Hashemi M, Ande SR, Yeganeh B, Xiao W, Eshraghi M, Bus CJ, Kadkhoda K, Wiechec E, Halayko AJ, *et al*: Apoptosis and cancer: Mutations within caspase genes. J Med Genet 46: 497-510, 2009.
29. Ahn MY, Kim TH, Kwon SM, Yoon HE, Kim HS, Kim JI, Kim YC, Kang KW, Ahn SG and Yoon JH: 5-Nitro-5'-hydroxyindirubin-3'-oxime (AGM130), an indirubin-3'-oxime derivative, inhibits tumor growth by inducing apoptosis against non-small cell lung cancer in vitro and in vivo. Eur J Pharm Sci 79: 122-131, 2015.